J Therm Anal Calorim (2012) 107:171–182
DOI 10.1007/s10973-011-1816-y

Applications of some thermo-analytical techniques to glasses and polymers

Arun Pratap · Kananbala Sharma

29th STAC-ICC Conference Special Chapter

Abstract Thermal characterization of materials provides conclusions regarding the identification of materials as well as their purity and composition, polymorphism, and structural changes. Analytical experimental techniques for thermal characterization comprise of a group of techniques, in which physical properties of materials are ascertained through controlled temperature program. Among these techniques, traditional differential scanning calorimetry (DSC) is a well-accepted technique for analyzing thermal transitions in condensed systems. Modulated DSC (MDSC) is used to study the same material properties as conventional DSC including: transition temperatures, melting and crystallization, and heat capacity. Further, MDSC also provides unique feature of increased resolution and increased sensitivity in the same measurement. "Hot disk thermal constant analyzer", based on Transient Plane Source (TPS) technique, offers simultaneous measurement of thermal transport properties of specimen, which are directly related to heat conduction such as thermal conductivity (λ) and thermal diffusivity (χ). This method enables the thermal analysis on large number of materials from building materials to materials with high thermal conductivity like iron. The temperature range covered so far extends from the liquid nitrogen point to 1000 K and should be possible to extend further. This review also presents some interesting results of phase transition temperature of miscible (CPI/TPI) and immiscible (PS/PMMA) polymeric systems carried out through dynamic mechanical analyzer along with the thermal transport properties obtained for *cis*-polyisoprene (CPI), *trans*-polyisoprene (TPI), and their blends determined by TPS technique.

Keywords Thermal properties · Modulated DSC · Transient plane source · Thermal conductivity · Thermal diffusivity · Dynamic mechanical analyzer · Phase transition temperature

A. Pratap (✉)
Condensed Matter Physics Laboratory, Applied Physics Department, Faculty of Technology & Engineering, The M. S. University of Baroda, Vadodara 390001, India
e-mail: apratapmsu@yahoo.com; apratapmsu@gmail.com

K. Sharma
Semiconductor and Polymer Science Laboratory 5-6, Vigyan Bhawan, Department of Physics, University of Rajasthan, Jaipur 302004, India
e-mail: kananbala18@yahoo.co.in; kananbala@gmail.com

Introduction

Glasses and polymers are condensed materials that support a number of technology and commercial thrust areas; photonics, clean energy and alternative energy sources, nanotechnology, thermal appliances, electrical insulation, and high performance composites used in aircrafts are a few to name. With the advent of bulk metallic glasses, it has become possible to use them in golf clubs and exploit other applications due to their extremely enhanced mechanical properties. These materials seamlessly integrate multidisciplinary research including chemist and chemical engineering, physicist, device engineers, biotechnologist, and bio-medical researchers. The tempestuous growth in the uses of polymers, glasses, and ceramics has provided a leading role in the development of thermo-analytical measuring techniques with a high degree of automation to assist the determination of important parameters necessary for the processing. An increasing knowledge of the structure and properties are facilitated by

these techniques including some important aspects about thermal stability, and temperature limits of applicability, aging and thermo-mechanical behavior, viscoelastic properties and processing conditions for shaping, casting, molding, and extrusion. Analytical experimental techniques for thermal characterization comprise a group of techniques, in which physical properties of materials are ascertained through controlled temperature program. Among these, some of the commonly used thermal characterization techniques are thermogravimetric analyzer (TG), differential thermal analyzer (DTA), differential scanning calorimeter (DSC), dynamical mechanical analyzer (DMA), and thermal constant analyzer (TCA) etc. Table 1 depicts the list of the physical properties measured from the above mentioned respective characterization techniques.

When a material system is subjected to heat energy, its interaction with matter can be measured in terms of the following thermal characteristic parameters like:

- Thermal conductivity.
- Thermal diffusivity.
- Specific heat.
- Thermal expansion.
- Thermo elasticity.
- Phase transformations.

These parameters are fundamental physical properties of both the scientific and technological interest, which are particularly important for construction materials used in a thermal environment, where heat transfer and insulation are of primary concern. Based on these, we will focus our attention toward these thermal characteristic parameters of the materials through DMA and hot disk thermal constant analyzer. DMA is frequently used to ascertain phase transition temperature of the material where as, Hot Disk Thermal Constant analyzer (based on transient plane source (TPS) technique) offers simultaneous measurement of thermal transport properties of specimen which are directly related to heat conduction such as thermal conductivity (λ), and thermal diffusivity (χ). DSC is a versatile thermal analysis technique used for about three decades to measure heat flows associated with transitions in materials as a function of temperature or time. DSC is widely used to provide quantitative and qualitative information about physical and chemical changes involving endothermic or exothermic processes or heat capacity changes.

Apart from the numerous advantages leading to its use in variety of areas like materials analysis, applicability to polymers and organic materials as well as various inorganic materials, pharmaceutical drugs; DSC does have some limitations. These limitations include the difficulty of optimum choice of heating range to get good resolution and good sensitivity simultaneously, difficulty in interpreting complex transitions (e.g. glass transition and enthalpic relaxation, melting and crystallization perfection), and measurement of heat capacity during a reaction.

Modulated DSC is a new improved technique and is an attempt toward overcoming most of the limitations of conventional DSC. Modulated DSC and MDSC is a patented [1] and commercialized [2] method invented by Dr. Mike Reading of ICI Paints (Slough, UK) and patented by TA instruments.

Numerical modeling and analysis of temperature modulated DSC has been recently carried out [3] on the separability of reversing heat flow from non-reversing heat flow to study heat capacity. In fact, one of the major advantages of the MDSC method is its ability to separate these reversing and non-reversible processes by the measurement of the contribution of reverse and non-reserve heat flows in total heat flow during a phase transition. Several studies have been reported for glass transitions and crystallization in polymers [4], chalcogenide glasses [5], and metallic glasses [6] by MDSC. But the study of the detailed crystallization process of an amorphous alloy using various kinetics equations is yet to be reported. Our recently reported study [7] on a three component transition metal based amorphous alloys viz. $Ti_{50}Cu_{20}Ni_{30}$ are among the first such publication. Recently, MDSC has been used quite effectively and extensively for investigating [8] thermodynamics of crystalline and amorphous phases of a new drug and vitrification and curing study [9]. Jinan Cao [10, 11] has carried out detailed mathematical studies of modulated DSC and has concluded that a quantitative separation of the kinetic and non-kinetic components is

Table 1 List of various thermal characterization techniques with the physical property ascertained through controlled temperature program.

Physical properties ascertained	Technique
Thermal stability/degradation, curing kinetics, phase transition measurement and pyrolysis kinetics	Thermogravimetric analyzer (TG)
Phase transition, thermal stability and kinetics of phase transition	Differential thermal analyzer (DTA)
Phase transition, thermal stability and kinetics of phase transition	Differential scanning calorimeter (DSC)
Phase transition, mechanical properties, viscosity, and activation energy	Dynamical mechanical analyser (DMA)
Thermal conductivity and thermal diffusivity	Thermal constant analyser (TCA)
Thermal expansion coefficient, phase transition, and density change	Thermal dilatometer

problematic. Besides, the quantitative determination of the heat capacity of a sample is rather difficult, if not impossible.

Theory

In modulated DSC, the same heat flux DSC cell arrangement is employed, but the heating profile applied to the sample and reference by furnace are different. The non-linear heating profile results from the sinusoidal modulation (oscillation) overlaid on the traditional linear ramp. The net effect of imposing more complex heating profile is just like running two experiments simultaneously in the following way:

1. One experiment at the traditional linear (underlying) heating rate; and
2. Another at a more rapid sinusoidal (instantaneous) heating rate (Fig. 1).

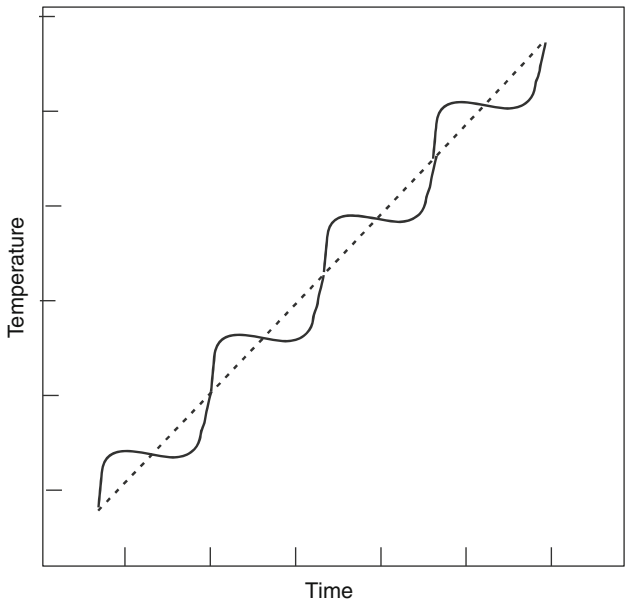

Fig. 1 Typical modulated temperature profile (*Dashed line* underlying heating rate).

The temperature in modulated DSC changes with time in a non-linear fashion given by

$$T(t) = T_0 + \beta t + A_T \sin\omega t \quad (1)$$

where T_0 is the starting temperature; t is the time (minutes); β is the linear heating rate (°C/min); A_T is the amplitude of temperature modulation (±°C); $\omega = 2\pi/p$; the modulation frequency ($\sec^{-1}$); p is the period (sec).

Consequently, the measured heating rate

$$\alpha = \frac{dT}{dt} = \beta + A_T \omega \cos\omega t \quad (2)$$

It is clear from Eq. 2 that the heating rate becomes non-linear due to the second oscillating term. The first term, β is the traditional linear (underlying) heating rate which improves resolution. On the other hand, the more rapid oscillating (instantaneous) rate expressed by the second term improves sensitivity. Thus, modulated DSC is a rare combination of high resolution and sensitivity in the same experiment (Figs. 2, 3, 4).

MDSC is claimed to have two crucial advantages over conventional DSC. The first one being the measurement of heat capacity in a simple run with accuracy higher than that of DSC. The relative sensitivity of MDSC for measurement of heat capacity is 5 times greater than DSC. The other benefit of MDSC is its ability to separate reversing and non-reversing components of an endotherm or exotherm which would have significant impact for thermal analysis of materials.

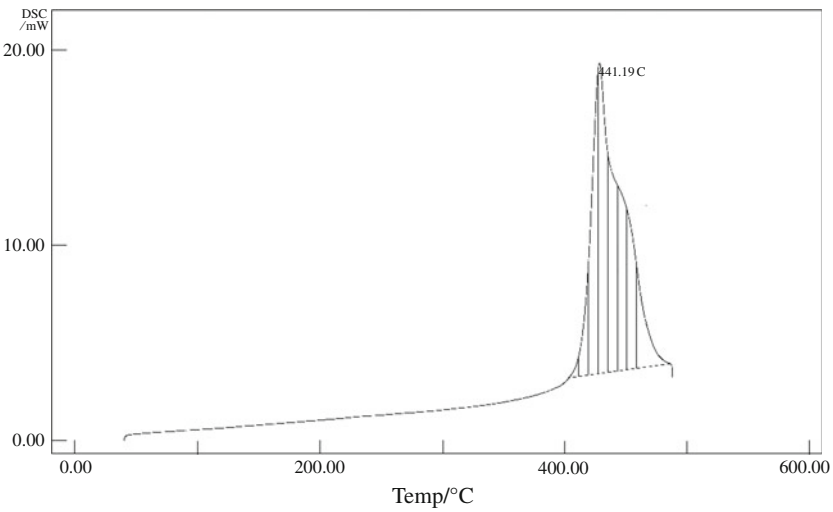

Fig. 2 Overlapping crystallization peaks of $Ti_{20}Zr_{20}Cu_{60}$ in DSC.

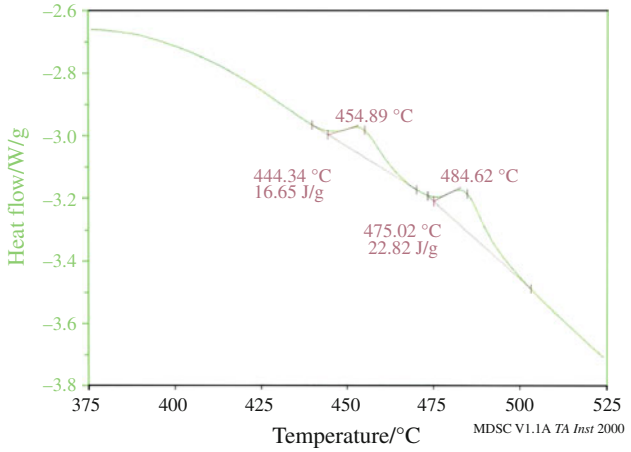

Fig. 3 Separation of overlapping crystallization peaks of $Ti_{20}Zr_{20}Cu_{60}$ in MDSC.

The instantaneous heat flow in a modulated DSC

$$\frac{dQ}{dT} = C_p(\beta + A_T\omega\, Cos\,\omega t) + f'(t,T) + A_k Sin\,\omega t \qquad (3)$$

where $(\beta + A_T\omega\cos\omega t) = \frac{dT}{dt}$ is measured heating rate; $f'(t,T)$ is the kinetic response without temperature modulation; A_k is the amplitude of kinetic response to temperature modulation.

The total heat flow consists of heat capacity-related (reversing) and kinetic (non-reversing) components. Average heat flow value is continuously calculated by Fourier transformation analysis of modulated heat flow signal. Heat capacity is calculated from the ratio of modulated heat flow amplitude to the product of amplitude of modulation temperature and frequency. The reversing heat flow is determined by multiplying this heat capacity with average heating rate. Events observed in the reversing heat flow are usually transitions, which are thermodynamically reversible at the time and temperature at which they are detected. Typical reversing events are glass transitions and crystalline melting. Thermal dehydration and decomposition have also been studied extensively [12, 13] using thermo-analytical techniques. On the contrary, non-reversible events are usually thermodynamically non-reversible at the time and temperature at which they are detected. Such non-reversible transitions are evaporation, decomposition, enthalpic relaxation, cold crystallization, thermo-set cure etc.

Applications

Glass transition

The conventional DSC has been extensively employed for studying the glass transition and crystallization. However, many metallic glasses have very small undercooling ($T = T_x - T_g$); where T_x is crystallization temperature and T_g is glass transition temperature. In such glasses, glass transitions are closely followed by crystallization and often the transitions are not observed by conventional DSC. The glass transition is a reversible process in which heat is absorbed to accommodate the heat capacity increase during the transition.

Many transitions are complex because they involve multiple processes. Enthalpic relaxation that occurs at the glass transition is an endothermic process that can vary in magnitude depending on the thermal history of the material. Under some circumstances, it can make the glass transition appear to be a melting transition. These problems get enhanced in analyzing blends of materials. Conventional DSC does not allow these complex transitions to be analyzed properly because it measures only the sum of all thermal events of the samples.

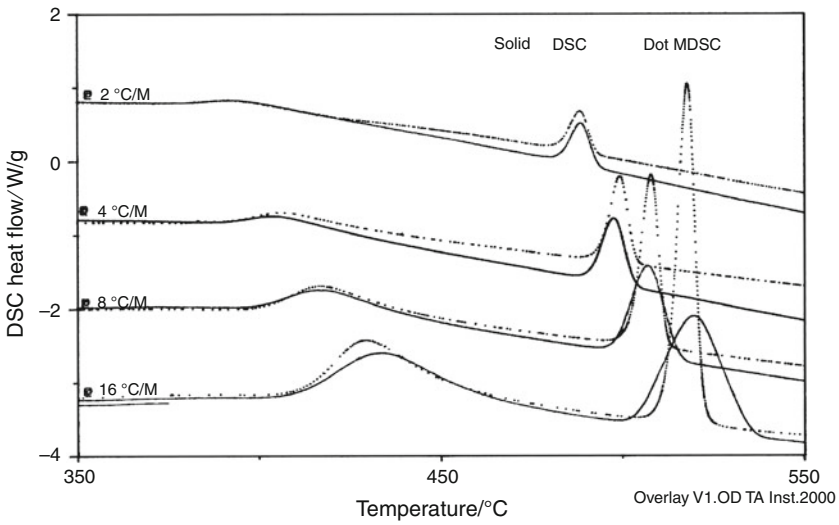

Fig. 4 Relative sensitivity of DSC and MDSC for crystallization.

Crystallization

Crystallization is a non-reversible exothermic process which releases heat. The experimental data on crystallization has been interpreted on the basis of the method of modified Kissinger's equation [14, 15] for determination of activation Energy and fractional crystallization method [16] for ascertaining mechanism. From the equation suggested [17] for non-isothermal crystallization, the activation energy for crystallization, E_c can be evaluated.

$$\ln[-\ln(1-x)] = -n\ln(\alpha) - 1.052\frac{mE_c}{RT} + \text{const.} \tag{4}$$

where x is the fractional crystallization, at any temperature T, heated at uniform rate and α is heating rate.

The equation of Matusita and Sakka given by Eq. 4 originates from the following expression:

$$[-\ln(1-x)] = \frac{k'}{\alpha^n}\exp\left(-\frac{mE}{RT}\right). \tag{5}$$

For MDSC, the measured heating rate becomes

$$\alpha = \frac{\mathrm{d}T}{\mathrm{d}t} = \beta + A_T\omega\cos\omega t \tag{6}$$

Here, β is the linear rate and the second term comes from sinusoidal temperature modulation. It is very essential to have positive heating profile through out the MDSC experiment. To achieve this and to avoid cooling, the following condition must be satisfied.

$$\beta \geq A_T\frac{2\pi}{p} \tag{7}$$

This condition enables to periodically achieve a 0 °C/min minimum instantaneous heating rate which, in turn, is required for two reasons. First, by not cooling the material any time during the modulation, the possibility for artificially affecting any crystallization phenomena is eliminated. Secondly and more importantly, when the heating rate is zero, there is no heat flow associated with heat capacity-related (reversing events), and hence any heat flow observed must be the result of kinetic phenomena.

Thus, the expression (5) changes to

$$[-\ln(1-x)] = \frac{k'}{(\beta + A_t\omega\cos\omega t)^n}\exp\left(-\frac{mE}{RT}\right). \tag{8}$$

The expansion of the term $(\beta + A_T\omega\cos\omega t)^n$ gives rise to the following expression:

$$(\beta + A_T\omega\cos\omega t)^n = \beta^n\left(1 + n\frac{A_T\omega}{\beta}\cos\omega t + \frac{n(n-1)}{2!}\frac{A^2\omega^2}{\beta^2}\cos^2\omega t + \ldots\right) \tag{9}$$

By taking the logarithm of Eq. 5, one gets

$$\ln[-\ln(1-x)] = -\ln(\beta + A_T\omega\mathrm{Cos}\omega t)^n - \frac{mE}{RT} + \text{const.} \tag{10}$$

Using Eq. 9 and taking the average over a complete cycle, Eq. 10 transforms to

$$\ln[-\ln(1-x)] = -\left[n\ln\beta + \ln\left\{1 + \frac{n(n-1)}{2!}\frac{A^2\omega^2}{\beta^2}\left(\frac{1}{2}\right) + \ldots\right\}\right] - \frac{mE}{RT} + \text{const}t. \tag{11}$$

Equation 11 can be rewritten as [15]

$$\ln[-\ln(1-x)] = -\ln\beta\left[n + \frac{n(n-1)}{4}\frac{A^2\omega^2}{\beta^2\ln\beta} + \ldots\right] - \frac{mE}{RT} + \text{const}t. \tag{12}$$

For $n = 1$, i.e. for surface crystallization, the expression for the fractional crystallization reduces to the original Matusita and Sakka expression given by Eq. 4. For one, two or three-dimensional nucleation, and the value of the exponent n will be less as compared with the subsequent value obtained from DSC results because the value of $\ln\beta$ in the denominator of the second term within parenthesis on R.H.S of Eq. 12 is negative.

For the evaluation of the activation energy of crystallization E_c, the modified Kissinger equation [16] is used and is given by the following expression

$$\ln\left(\frac{\alpha^n}{T_p^2}\right) = -\frac{mE_c}{RT_p} + \ln K \tag{13}$$

where the shift in peak crystallization temperature T_p with heating rate α is used to determine E_c and m is dimensionally of growth.

In temperature modulated DSC, the measured heating rate is non-linear given by Eq. 2. Putting the value of α from Eq. 2 in the modified Kissinger Eq. 13, we get

$$\ln\left(\frac{\beta^n}{T_P^2}\right) + \frac{n(n-1)}{4}\frac{A_T^2\omega^2}{\beta^2} + \ldots = -\frac{m'E_c}{RT_P} + \ln K \tag{14}$$

where β is linear heating rate. The second term on the RHS of Eq. 14 is expected to cause non-linearity in the modified Kissinger plot of modulated DSC results. However, it is observed that the points of $\ln\left(\frac{\beta^n}{T_P^2}\right)$ versus $\frac{1}{T_P}$ lie on straight line. So, we may not consider the effect of the second term. The activation energy of crystallization obtained in such a way is termed as apparent activation energy.

Using the value of the apparent order parameter n' and $m' = n'-1$, E_c, the apparent activation energy of crystallization is computed from the slope of $\ln\left(\frac{\beta^{n'}}{T_P^2}\right)$ versus $\frac{1}{T_P}$ plots.

Dynamic mechanical analyzer (DMA)

Dynamic mechanical analyzer is a sensitive technique that characterizes the mechanical response of materials by monitoring property change with respect to the temperature and frequency of applied sinusoidal stress. It is used to

(i) Detect transitions arising from molecular motions or relaxations.
(ii) Determine mechanical properties, i.e. modulus, damping of viscoelastic materials over spectrum of time and temperature.
(iii) Develop structure property or morphology relationships.

Theory and instrumentation of DMA

The instrument operation is relatively simple to understand. In this instrument, a sinusoidal force (stress) with a defined frequency is applied to the sample through the motor. The stress is transmitted though the device shaft onto the sample, which is mounted in a clamping mechanism. As the sample deforms, the amount of displacement is measured by linear variable differential transformer (LVDT) positional sensor. The strain can be calculated from the displacement. The magnitude of the applied stress and the resultant strain are used to calculate the stiffness of the material under stress (Fig. 5). The phase lag between the two (or δ) is used to determine Tan δ, the damping factor. On the basis of phase lag (δ) observed by DMA, there are three classes of materials [18]: For perfectly elastic materials like steel the phase angle is zero ($\delta = 0°$) and for purely viscous materials such as a liquid, the phase angle is 90°. Viscoelastic materials fall in between these two extremes, i.e. $0° < \delta < 90°$. Most polymers exhibit this behavior and have an elastic and viscous component.

When the sample is subjected to sinusoidal stress, it is deformed sinusoidally within linear viscoelastic region. The stress applied to the material at any time t is

$$\sigma = \sigma_0 \sin\omega t \tag{15}$$

where σ is stress at any time, σ_0 is maximum stress at the peak of sine wave, ω is frequency of oscillation, and t is time.

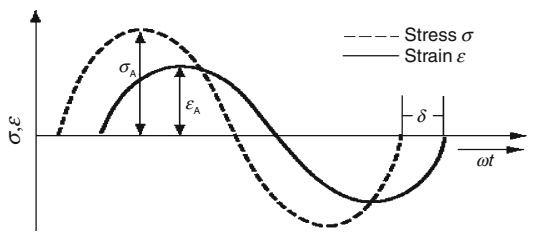

Fig. 5 Sinusoidal oscillation and response of a material.

The rate of variation of stress with respect to time is given by

$$d\sigma/dt = \omega\sigma_0 \cos\omega t \tag{16}$$

The resulting strain wave depends upon the extent of elastic and viscous behavior exhibited by the material. Therefore, strain at any time t is

$$\varepsilon(t) = \sigma/E = \sigma_0 \sin\omega t/E$$

Therefore,

$$\varepsilon(t) = \varepsilon_0 \sin\omega t$$

where E is the modulus and ε_0 is the strain at maximum value of stress.

The phase lag between the applied stress and resultant strain is an angle $\delta = \pi/2$ for viscous material. i.e.

$$\varepsilon(t) = \varepsilon_0 \sin(\omega t + \delta)$$

or

$$\varepsilon(t) = \varepsilon_0[\sin\omega t\cos\delta + \cos\omega t\sin\delta] \tag{17}$$

Here,

$$\varepsilon' = \varepsilon_0 \sin\delta$$

and

$$\varepsilon'' = \varepsilon_0 \cos\delta$$

Therefore, the complex strain of material is as follows

$$\varepsilon^* = \varepsilon' + i\varepsilon''$$

and complex modulus of a material,

$$E^* = E' + iE''$$

Hence,

$$E' = \sigma_0/\varepsilon' = \sigma_0/\varepsilon_0 \sin\delta \tag{18}$$

and

$$E'' = \sigma_0/\varepsilon'' = \sigma_0/\varepsilon_0 \cos\delta \tag{19}$$

By comparing Eqs. 18 and 19, we get

$$\begin{aligned} E'' &= E'\varepsilon_0 \sin\delta/\varepsilon_0 \cos\delta \\ E''/E' &= \mathrm{Tan}\delta \end{aligned} \tag{20}$$

where Tanδ is the damping factor, which is an indicator of how efficiently the material loses energy in molecular arrangements and internal friction.

A dynamic mechanical analyzer is often referred to as DMTA (dynamic mechanical thermal analyzer) as during the measurement, the temperature of the sample is defined and can be changed. The sample can be mounted in the DMA in a number of ways depending on the characteristics of the sample material. The six common geometries are: single cantilever bending, dual cantilever bending, three

point bending, tension, compression, and shear. Sample stiffness depends upon the modulus of elasticity and geometry. In this technique, the measured modulus depends upon the choice of geometry i.e. tension, compression and bending mode yields the Young's (E^*), and shear (torsion) mode gives the shear modulus.

The temperature that corresponds to a maximum in Tan δ versus temperature curve has been considered as "phase transition temperature (T_g)" for the polymeric blend samples. The phase transition temperature (T_g) is a temperature boundary almost for all amorphous polymers (and many crystalline polymers) above which the substance remains soft, flexible, and rubbery and below which it becomes hard, brittle, and glassy. The phase transition temperature (T_g) of a polymer material is correlated with the segmental motion of the polymer chains. It is an important parameter for a polymeric material. It is used as a measure for evaluating the flexibility of a polymer and the type of response the polymeric material would exhibit to mechanical stress. The T_g of a polymer, therefore, decides whether a polymer at the 'use temperature' will behave like rubber or plastic. In this way, it helps in choosing the right processing temperature, i.e. the temperature region in which the material can be converted into finished product through different processing techniques such as molding, calendaring, and extrusion. In the study of polymer blends these factors are considered for industrial interest, due to the synergic effects of mixing a commercially available component to enhance properties such as processability and end-use characteristic, the knowledge of T_g value is very essential. DMA is estimated to be 100 times more sensitive to the glass transition than DSC [19]. It can resolve other more localized transitions not detected in DSC [20]. In addition, this technique allows the rapid scanning of a material's modulus and viscosity as a function of temperature or frequency.

Hot disk thermal constants analyzer

The thermal transport properties such as thermal conductivity (λ) and thermal diffusivity (χ) are important in ascertaining the processing conditions as well as the applications of polymeric materials. This method enables the thermal analysis on large number of materials from building materials to materials with high thermal conductivity like iron. The temperature range covered so far extends from cryogenic to high temperatures (1000 K) and should be possible to extend further. It can measure thermal conductivities between 0.01 and 500 W/mK.

The hot disk thermal constant analyzer is based on Transient Plane Source (TPS) method. TPS method is a transient method, which is an extension of the transient hot strip method (THS) and initially introduced by Gustafsson [21]. In transient method, the sample has to be taken to be at thermal equilibrium with the surroundings and then one end of the sample is subjected to a transient heat pulse. The change in temperature is monitored at different points of time of measurement. By using the measured values of temperature variation and with the help of the solution of the differential heat equation the thermal diffusivity (χ) and thermal conductivity (λ) can be evaluated [22].

The advantage of using TPS method over the other transient method is that the hot wire (THW) and hot strip (THS) methods require long samples since the resistivity of a resistance thermometer is directly proportional to the initial resistance of the wire or the strip. In order to obtain a reasonably high initial resistance of the sensor element and at the same time to be able to work with a convenient and compact configuration of the sample, the hot disk sensor has been designed to minimize the total size of the sample. Other advantage of using TPS method over THS method is better protection, better electrical contacts, and repeated use of sensor.

The temperature dependence of the thermal conductivity and thermal diffusivity of polymers is also of scientific interest both from the practical standpoint as it entails establishing the mechanism of heat conduction in polymers in different states. Thermal conductivity describes the ability of materials to transport heat while thermal diffusivity is the thermophysical parameter, which characterizes the rate of temperature diffusion in the material due to heat flux in the non-steady state. It is familiarly known that the thermal conductivity and diffusivity of polymers vary extensively depending on the structure, density, porosity, molecular weight, orientations, and other structural features of the material [23]. These properties also exhibit a strong dependence toward temperature, pressure, and environmental condition. The heat conduction in polymeric materials is mainly caused through phonons. On the microscopic level, thermal conductivity and thermal diffusivity are colligated to the distribution function of these phonons of a given material as well as to the average phonon velocity and their mean-free path between successive collisions.

Theory of transient plane source method

In this method, the transient plane source element behaves both as a source of heat given to the sample and as a sensor of temperature increase in the sample. The TPS element consists of an electrical conducting pattern of thin nickel foil (10 μm) in the form of double spiral, which resembles a hot disk, embedded in an insulating layer made of kapton (70 μm) or mica depending upon their use in low, room, and high temperature respectively.

For the measurement of thermal constants-λ, χ, and ρc_p of the sample material the sensor is sandwiched between identical plane surfaces of the test samples. Size of the sample should be such that the distance from the hot disk (conducting pattern) to the nearest sample boundary is larger than the probing depth Δp [24], which can be defined as

$$\Delta p = \beta(\chi t_{\max})^{1/2} \tag{21}$$

where $t_{\max}$ is the total time of the transient recording; χ is the thermal diffusivity of sample under test; β is the constant of the order of unity and related to the experimental accuracy.

If R_0 is the initial resistance of hot disk, and α is the temperature coefficient of resistance of the nickel foil then after applying a constant electrical power to the sensor, the increase in temperature $\Delta T(\tau)$ can be calculated using the equation

$$R(t) = R_0\left[1 + \alpha\,\overline{\Delta T(\tau)}\right] \tag{22}$$

where $R(t)$ is the variation in the sensor resistance with time and $\overline{\Delta T(\tau)}$ is a properly calculated mean value of the time dependent temperature increase of the TPS element.

Let us consider an infinite solid with a thermal conductivity λ, a thermal diffusivity χ, and specific heat per unit volume ρc_p. If conducting pattern (sensor) is located in the yz plane inside this solid, the temperature increase, at a point y, z and the time t, due to an output of power Q per unit area is given by

$$\Delta T(y,z,t) = \frac{1}{8\pi^{3/2}\rho c}\int_0^t \mathrm{d}t'\,[\kappa(t-t')]^{-3/2} \times \int_A \mathrm{d}y'\mathrm{d}z' Q[y',z',t'] \exp\left\{-\left[(y-y')^2 + (z-z')^2\right] \times [4\kappa(t-t')]^{-1}\right\} \tag{23}$$

where A is the total area of the conducting pattern.

For convenience, the temperature increase can be expressed as a function of τ, which is defined as

$$\tau = [t/\theta]^{1/2},\ \theta = a^2/\chi \tag{24}$$

where t is the time measured from the start of the transient heating, a is the radius of hot disk, and θ is the characteristic time.

Using Eq. 24 and taking $\chi(t-t') = \sigma^2 a^2$, Eq. 23 can be written as

$$\Delta T(y,z,\tau) = \frac{1}{4\pi^{3/2}a\lambda}\int_0^{\tau a}\sigma^{-2}\mathrm{d}\sigma \int_A \mathrm{d}y'\mathrm{d}z' Q\left[y',z',t-\frac{\sigma^2 a^2}{\chi}\right] \times \exp\left[-\frac{(y-y')^2+(z-z')^2}{4\sigma^2 a^2}\right] \tag{25}$$

where $\chi = \lambda/\rho c_p$, ρ is the density of material of the sample, σ is a constant variable

If it is assumed that the disk contains a number 'm' of concentric ring sources, an exact solution of Eq. 24 from ring source solution immediately becomes

$$\overline{\Delta T(\tau)} = \frac{P_0}{\pi^{\frac{3}{2}}a\lambda} D_{\mathrm{S}}(\tau) \tag{26}$$

where P_0 is the total output power and $D_s(\tau)$ is the geometric function given by the relation

$$D_{\mathrm{s}}(\tau) = [m(m+1)]^{-2} \times \int_0^{\tau}\frac{\mathrm{d}\sigma}{\sigma^2}\left[\sum_{l=1}^{m} l\left\{\sum_{k=1}^{m} k.\mathrm{Exp}\left(\frac{(-l^2-k^2)}{2\,\sigma^2\,m^2}\right)\right\} L_0\left(\frac{lk}{2\,\sigma^2\,m^2}\right)\right] \tag{27}$$

in which L_0 is the modified Bessel function and l, k are the dimension of the resistive pattern.

To record the potential difference variations, which normally are of the order of a few millivolts during the transient recording, a simple bridge arrangement as shown in Fig. 6 has been used. If we assume that the resistance increase will cause a potential difference variation $\Delta U(t)$ measured by the voltmeter in the bridge, the analysis of the bridge indicates that

$$\Delta E(t) = \frac{R_{\mathrm{s}}}{R_{\mathrm{s}}+R_0} I_0 \Delta R(t) = \frac{R_{\mathrm{s}}}{(R_{\mathrm{s}}+R_0)} \frac{I_0 \alpha R_0 P_0}{\pi^{3/2} a\lambda} D_{\mathrm{s}}(\tau) \tag{28}$$

where

$$\Delta E\,(t) = \Delta U(t)[\,1 - C.\Delta U(t)]^{-1} \tag{29}$$

and

$$C = \frac{1}{R_{\mathrm{S}} I_0\left[1 + \frac{\gamma R_{\mathrm{P}}}{\gamma(R_{\mathrm{S}}+R_0)+R_{\mathrm{P}}}\right]} \tag{30}$$

Here, R_{p} is the lead resistance, R_{s} is a standard resistance with a current rating that is much higher than I_0, which is the initial heating current through the arm of the bridge containing the TPS element. γ is the ratio of the resistances

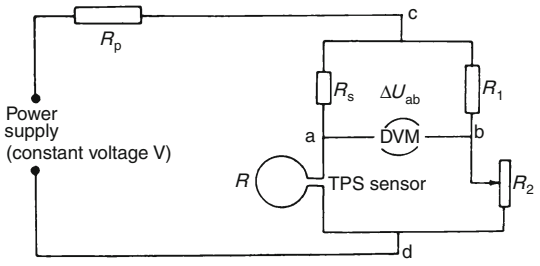

Fig. 6 Bridge circuit diagram of TPS technique.

in two ratio arms of the bridge circuit, which is taken to be 100 in the present experiment.

Calculating $D_s(\tau)$ using a computer program and recording the change in potential difference $\Delta U(t)$, one can determine λ. Similarly, diffusivity χ can be determined by finding the values of θ from the transient event.

Many polymers and polymeric blends have been characterized in this aspect by the author and her group in the last decade. This study also presents some interesting results of phase transition temperature of miscible (CPI/TPI) and immiscible (PS/PMMA) polymeric systems carried out through dynamic mechanical analyzer along with the thermal transport properties obtained for cis-polyisoprene (CPI), trans-polyisoprene (TPI) and their blends determined by TPS technique.

Results

Phase transition temperature study of miscible blends

In order to investigate phase behavior of CPI, TPI and their blends,DMA has been adequately used in the present study. In Fig. 7, Tan δ versus temperature curves are plotted for ease of glass transition detection, assignment, and comparison. The plots of Tan δ against temperature show well-defined and symmetric peaks corresponding to the relaxation associated to the transition from glassy state to the elastic state of the rubber. The characteristic temperature corresponding to the peak point is identified as glass transition temperature T_g [25]. All the blends show a single glass transition temperature, which confirms that all the blends are miscible as reported by other researchers [26, 27] also. It is observed from this figure that the glass transition temperature shows increasing trend with increasing TPI content. This behavior can be explained on the basis of crosslink density. As the concentration of TPI increases, crosslink density also increases [28] and therefore, a rigid structure is produced due to the lower molecular weight between crosslink. As a result, there is a shifting in the transition (T_g) to lower temperature. Moreover, It is reported [29] that the glass transition temperature depends upon crystallinity. So this can also be explained on the basis of WAXS measurements. An increase in TPI concentration increases the crystallinity [30] and as a result T_g is shifted to lower side.

Phase transition temperature study of immiscible blend

In Fig. 8, Tanδ versus temperature curves are plotted for ease of glass transition detection, assignment, and comparison. The T_g of pure PS and pure PMMA was observed to be 113.1 and 78.8 °C, respectively. These values depend on molecular weight and agree with the literature values for similar polymers [31].The blends of PS/PMMA demonstrate similar two well-defined peaks over the studied composition range. In Fig. 8b–d the first peak observed at lower temperatures corresponds to pure PMMA phase while the peak exhibited at higher temperature suggests the presence of PS phase. The T_g values corresponding to PS and PMMA phases for all samples are as tabulated in Table 2.

It has also been found that the T_g corresponding to PMMA phase shifts toward the higher temperature with the increase of PS concentration and highest T_g value of PMMA phase is obtained for 70PS/30PMMA blend. On the other hand, the T_g of PS phase is observed nearly constant with slight shifting of T_g toward lower temperature side as the PMMA concentration is made to increase in PS/PMMA blend series. Such behavior suggests that the phase interaction between PS and PMMA are physical, not chemical, and are dependent on changes in morphology that accompany the composition changes (Table 2).

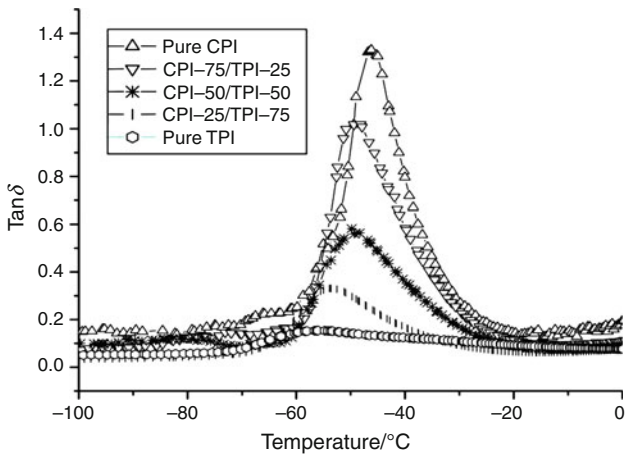

Fig. 7 Tan δ versus Temperature curve of CPI/TPI blends.

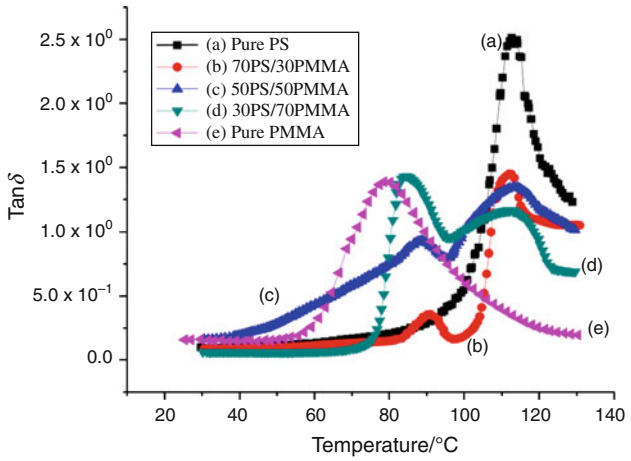

Fig. 8 Variation of Tan δ versus Temperature of studied samples.

Table 2 Glass transition temperature of PS/PMMA polymeric blend samples.

Sample	Glass transition temperatures			
	Experimental		Mean $T_{g(M)}$/°C	Theoretical $T_{g(P)}$/°C
	T_g-*I*/°C (PMMA phase)	T_g-*II*/°C (PS phase)		
Pure PS	113.1			
70PS/30PMMA	90.5	112.3	101.4	105.76
50PS/50PMMA	88.4	113.8	101.1	101.1
30PS/70PMMA	84.1	112.7	98.4	104.12
Pure PMMA	Single T_g peak at 78.8			

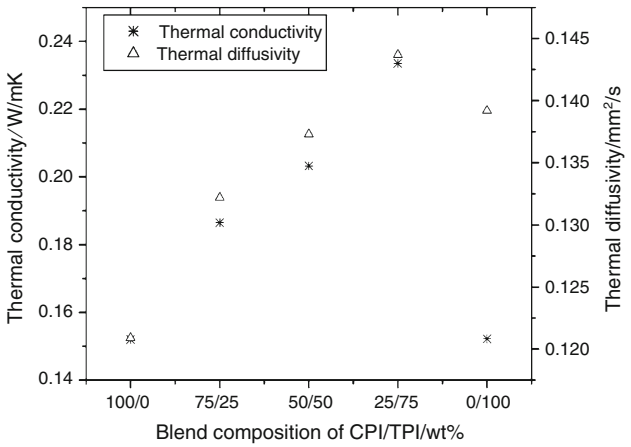

Fig. 9 Thermal conductivity and thermal diffusivity versus blend composition.

The existence of two well-defined T_g peaks corresponding to PMMA and PS phases respectively, in PS/PMMA blends with statistically constant T_g value of PS phase clearly reveals the fact that PS/PMMA polymeric blends are highly immiscible over the studied composition range.

The data shows that PMMA phase undergoes glass transition stage first, and so the crystallization process of this phase tends to occur primarily and initiates significant volume reduction and shrinkage, much more in the presence of number of PS domains. This differential shrinkage causes the PS phase to exert isotropic hydrostatic pressure on the PMMA phase, the available free volume is reduced, the ability of the polymer chains to attain the critical free volume is constrained, and the resultant glass structure of PMMA phase tends to attain at a comparatively higher temperature than pure state.

PMMA appears in viscous phase at about 110 °C, whereas PS phase is about to undergo transitions to glassy phase, and the T_g of the PS phase is observed to remain unaffected by the presence of the PMMA phase in all samples. This can be understood from the perspective of image analysis and morphologies of PS/PMMA blends. Interestingly, the dispersed PMMA phase has pulled away from the PS matrix during crystallization, presumably due to the differential shrinkage and incompatibility between PS and PMMA phases. This eliminates the possibility of compression effects of PMMA phase on the T_g of PS phase.

Thermal conductivity and thermal diffusivity of CPI, TPI and their blends

Figure 9 shows the thermal conductivity and thermal diffusivity values plotted against composition of the CPI/TPI blends. Thermal conductivity of pure CPI and Pure TPI are almost equal. As the concentration of TPI increases in the CPI/TPI blend thermal conductivity increases. This fact can be explained on the basis of crystallinity and crosslink density. It has been reported [32] that an increase in crystallinity increases the thermal conductivity. In the present samples, an increase in the TPI content of CPI/TPI blend increases both crystallinity and crosslink density which, in turn, increases the thermal conductivity of the samples. This is due to the fact that an increase in crosslink density decreases the average distance between the crosslinks. Further, increment in crosslink density reduces the average distance between crosslinks or chains up to a certain limit and after this limit a stage comes, when these crosslinks or chains unite together resulting in an abrupt increase of the average distance between them [33].

According to Berman et al. [34], if the average distance between the crosslinks is less than the range of elastic disorder (10 Å), thermal conductivity continuously increases with increasing crosslink density (which is in the case of CPI-75-TPI-25, CPI-50-TPI-50, and CPI-25-TPI-75 blends). In a case where average distance between crosslinks is greater than the range of elastic disorder, thermal conductivity is seen to decrease with increasing crosslink density (which is the case of pure TPI). Morgan and Scovell [35] proposed a postulate to this phenomenon. They postulated the existence of one-dimensional wave packets, which travel along the chains and have long mean-free paths. The wave packets may be scattered by chain

ends, crosslinks or interactions with other molecules, which reduces the thermal conductivity. Thermal diffusivity (χ) of the blends exhibit the same trend as obtained in the case of the thermal conductivity values, showing the proportionality between λ and χ.

Conclusions

Modulated DSC provides a powerful enhancement to the standard DSC experiment. MDSC has the unique combination of increased sensitivity and increased resolution. It provides simultaneously the heat flow as well as heat capacity in a single experiment. However, one feels that the choice of optimum MDSC conditions are not unique for all the thermodynamic processes (i.e. reversible and non-reversible) like glass transition, crystallization, melting etc. Hence, one has to be very careful in choosing the parameters of modulation corresponding to a particular process.

Besides, the present study suggests that thermal analysis techniques particularly, DMA and TPS are extremely useful in materials processing and characterizations. DMA is very sensitive to the motions of the polymer chains and it is a powerful tool for measuring transitions in polymers. It provides valuable information regarding phase transition temperature and conclusions toward miscibility of the polymeric blend system. For example, the phase transition study of CPI/TPI blends reveals that all the studied polymeric blend compositions exhibit single well-defined peaks. This shows that the blends of CPI with TPI are highly miscible system at all composition while, the phase transition study of PS/PMMA blends reveals that all the studied polymeric blend compositions exhibit two well-defined peaks and the T_g of PMMA phase gets changed as a function of the composition, whereas T_g of PS phase remains about constant statistically. This resolved that the blends of PS with PMMA are highly immiscible system.

On the other hand, TPS technique is also one of the versatile techniques for the precision of thermal transport properties of the material. The advantage of using TPS method over other transient method is that the conductivity pattern can be laid down such that the total electric resistance of the TPS element is much higher than that of the hot strip of THS method, while the sample size may be kept as small as 10 cc. Other advantages of using TPS sensor over THS methods are the better protection, better electrical contacts, and repeated use of the sensor. In case of CPI, TPI, and CPI/TPI blends, the thermal transport properties-thermal conductivity and thermal diffusivity are increased with increasing TPI content. However, pure TPI shows lower thermal properties than that of the blends but higher than that of pure CPI. This variation in thermal transport properties confirms that not only crystallinity, but also crosslink density and effective average chain length are responsible for these properties.

Acknowledgements The authors are grateful to I.U.C. for DAE facilities, Indore for providing the modulated DSC (TA Instruments, 2920) for experimentation on various amorphous alloys.

References

1. Reading Mike. US Patent Nos. B1 5,224,775; 5,248,199; 5,335,993;5,346,306.
2. Gill PS, Sauerbrunn SR, Reading M. Modulated differential scanning calorimetry. J Therm Anal. 1993;40:931–9.
3. Xu SX, Li Y, Feng YP. Numerical modeling and analysis of temperature modulated differential scanning calorimetry: on the separability of reversing heat flow from non- reversing heat flow. Thermochim Acta. 2000;343:81–8.
4. Boller A, Schick C, Wunderlich B. Modulated differential scanning calorimetry in the glass transition region. Thermochim Acta. 1995;266:97–111.
5. Wagner T, Kasap SO. Glass transformation, heat capacity and structure of As_x Se_{1-x} glasses studied by modulated temperature differential scanning calorimetry experimets. Phil Mag B. 1996; 74:667–80.
6. Li Y, Ng SC, Lu ZP, Feng YP, Lu K. Separation of glass transition and crystallization in metallic glasses by temperature-modulated differential scanning calorimetry. Phil Mag Lett. 1998;78:213–20.
7. Arun Pratap, Raval KG, Awasthi AM. Kinetics of crystallization of a ternary titanium based amorphous alloy. Mater Sci Engg A. 2001;304–306:357–61.
8. Bruni G, Milanese C, Berbenni V, Sartor F, Villa M, Marini A. Crystalline and amorphous phases of a new drug. J Therm Anal Calorim. 2010;102:297–303.
9. Gracia-Fernandez CA, Davies P, Gomez-Barreiro S, Lopez Beceiro J, Tarrio-Saavedra J, Artaga R. A vitrification and curing study by simultaneous TMDSC-photocalorimetry. J Therm Anal Calorim. 2010;102:1057–62.
10. Cao J. Mathematical studies of modulated differential scanning calorimetry II. Kinetic and non-kinetic components. Thermochim Acta. 1999;325:89–95.
11. Cao J. Mathematical studies of modulated differential scanning calorimetry I. Heat capacity measurements. Thermochim Acta. 1999;325:101–9.
12. Verma RK, Verma L, Chandra M, Verma BP. Kinetic parameters of thermal dehydration and decomposition from thermoanalytical curves of zinc dl-lactate. J Indian Chem Soc. 1998;75:162–4.
13. Verma RK, Verma L, Chandra M. Thermoanalytical studies on the non-isothermal dehydration and decomposition of dl-lactates of a series of transition metals. Indian J Chem. 2003;42A:2982–7.
14. Kissinger HE. Reaction kinetics in differential thermal analysis. Anal Chem. 1957;29:1702–6.
15. Matusita K, Sakka S. Kinetic study of crystallization of glass by differential scanning calorimetry. Phys Chem Glasses. 1979;20: 81–4.
16. Matusita K, Sakka S. Kinetic study on crystallization of glass by differential thermal analysis-criterion on application of Kissinger plot. J Non-Cryst Solids. 1980;38–39:741–6.
17. Raval KG, Lad Kirit N, Pratap A, Awasthi AM, Bhardwaj S. Crystallization kinetics of a multicomponent Fe-based amorphous alloy using modulated differential scanning calorimetry. Thermochimica Acta. 2005;425:47–57.
18. Nahm S. Use of dynamic mechanical analysis in thermoset resin development for composite applications. Composites convention and trade show 2001, Florida, USA.

19. Menard K. Dynamic mechanical analysis: a practical introduction. 2nd ed. U. S. A.: CRC Press; 1999.
20. Dixit M, Gupta S, Mathur V, Sharma K, Saxena NS. Activation energy of α- and β- relaxation process of PMMA and CdS-PMMA nanocomposite. J Nanostructured Polym Nanocomposite. 2009;6:28–35.
21. Gustafsson SE, International Patent Appl No PCT/SE 89/100137.
22. Gustafsson SE. Transient plane source techniques for thermal conductivity and thermal diffusivity measurements of solid materials. Rev Sci Instrum. 1991;62:797–804.
23. Lopes AMA, Felisberti IM. Thermal conductivity of PET/(LDPE/AI) composites determined by MDSC. Polym Testing. 2004;23:637–43.
24. Gustafsson SE, Karawacki E, Chohan Mohammad A. Thermal transport studies of electrically conducting materials using the transient hot-strip technique. J Phys D Appl Phys. 1986;19:727–35.
25. Baboo M, Dixit M, Sharma KB, Saxena NS. The structure and thermomechanical properties of blends of trans-polyisoprene with cis-polyisoprene. Int J Polym Mater. 2009;58:636–46.
26. Manzur A. Strain-induced crystallization in *cis*- and *trans*-polyisoprene blends: apparent crystallinity. J Macromol Sci Phys B. 1989;28:329–37.
27. Bochathum P, Chuwnawin S. Vulcanization of *cis*- and *trans*-polyisoprene and their blends: crystallization characteristics and properties. Euro Polym J. 2001;37:429–34.
28. Boochathum P, Prajudtake W. Vulcanization of *cis*- and *trans*-polyisoprene and their blends: cure characteristics and crosslink distribution. Euro Polym J. 2001;37:417–27.
29. Arvanitoyannis I, Kolokuris I, Nakayama A, Aiba S-I. Preparation and study of novel biodegradable blends based on gelatinized starch and 1, 4-*trans*-polyisoprene (gutta percha) for food packaging or biomedical applications. Carbohyd Polym. 1997;34:291–302.
30. Baboo M, Dixit M, Sharma K, Saxena NS. Effect of blending on mechanical and thermal transport properties of *cis*-polyisoprene with trans-polyisoprene. Polymer bulletin 2010; doi:10.1007/s00289-010-0378-7.
31. Mark JE. Polymer data handbook. New York: Oxford University Press; 1999.
32. Jayasree TK, Predeep P, Agarwal R, Saxena NS. Thermal conductivity and thermal diffusivity of thermoplastic elastomeric blends of styrene butadiene rubber/high density polyethylene: effect of blend ratio and dynamic crosslinking. Trends in Applied science Research. 2006;1:278–91.
33. Evseeva LE, Tanaeva SA. Thermophysical properties of epoxy composite materials at low temperatures. Cryogenics. 1995;35:277–9.
34. Berman BL, Madding RP, Dellinger JR. Effect of crosslinking on the thermal conductivity of polystyrene between 0.3 K and 10 K. Phys Lett A. 1969;30:315–6.
35. Morgan GJ, Scovell PD. Effective conductivity of short carbon fiber-reinforced polychloroprene rubber and mechanism of conduction. Polym Lett. 1977;15:193.